

Development and characterisation of *in vitro* human oral mucosal equivalents derived from immortalised oral keratinocytes

Luke R. Jennings^{1^*}, Helen E. Colley^{1^*} Ph.D, Jane Ong² Ph.D, Foti Panagakos² Ph.D, James G.

Masters² Ph.D, Harsh M. Trivedi² Ph.D, Craig Murdoch^{1*} Ph.D and Simon Whawell¹ Ph.D

¹School of Clinical Dentistry, University of Sheffield, Sheffield, S10 2TA, UK.

²Colgate-Palmolive Co., 909 River Road, Piscataway, NJ 08854, USA.

[^]These authors are joint first author.

* Corresponding author: Dr Craig Murdoch, University of Sheffield School of Clinical Dentistry, Claremont Crescent, Sheffield, S10 2TA, UK, Tel: +44 (0)114 22 65458, Fax: +44 (0)114 271 7863, e-mail: s.whawell@sheffield.ac.uk

Mr Luke R Jennings, University of Sheffield School of Clinical Dentistry, Claremont Crescent, Sheffield, S10 2TA, UK, Tel: +44 (0)114 226 5458, Fax: +44 (0)114 271 7863, e-mail: l.jennings@sheffield.ac.uk

Dr Helen E Colley, University of Sheffield School of Clinical Dentistry, Claremont Crescent, Sheffield, S10 2TA, UK, Tel: +44 (0)114 226 5458, Fax: +44 (0)114 271 7966, e-mail: h.colley@sheffield.ac.uk

Dr Jane Ong, Colgate-Palmolive Company, 909 River Road, Piscataway, NJ 08855-1343, USA.
Tel: +00 732 878 7731. Jane_ong@colpal.com

Dr Harsh M. Trivedi, Colgate-Palmolive Company, 909 River Road, Piscataway, NJ 08855-1343, USA. Tel: +00 732 878 7731. harsh_m_trivedi@colpal.com

Dr James G Masters, Colgate-Palmolive Company, 909 River Road, Piscataway, NJ 08855-1343, USA. Tel: +00 732 878 7633. jim_masters@colpal.com

Dr Foti Panagakos, Colgate-Palmolive Company, 909 River Road, Piscataway, NJ 08855-1343, USA. Tel: +00 732 878 7213. foti_panagakos@colpal.com

Dr Simon Whawell, University of Sheffield School of Clinical Dentistry, Claremont Crescent, Sheffield, S10 2TA, UK, Tel: +44 (0)114 2717953, Fax: +44 (0)114 271 7863, e-mail: s.whawell@sheffield.ac.uk

Abstract

Tissue engineered oral mucosal equivalents (OME) are being increasingly used to measure toxicity, drug delivery, and to model oral diseases. Current OME are mainly comprised of normal oral keratinocytes (NOK) cultured on top of a normal oral fibroblasts (NOF)-containing matrix. However, the commercial supply of NOK is limited, restricting widespread use of these mucosal models. In addition, NOK suffer from poor longevity and donor-to-donor variability. Therefore, we constructed, characterised and tested the functionality of oral mucosal equivalents based on commercial TERT2-immortalised oral keratinocytes (FNB6) in order to produce a more readily available alternative to NOK-based OME. FNB6 OME cultured at an air-to-liquid interface for 14 days exhibited expression of differentiation markers cytokeratin 13 in the suprabasal layers and cytokeratin 14 in basal layer of the epithelium. Proliferating cells were restricted to the basal epithelium and there was immuno-positive expression of E-cadherin confirming the presence of established cell-to-cell contacts. The histology and expression of these structural markers paralleled those observed in the normal oral mucosa and NOK-based models. Upon stimulation with TNF α & IL-1, FNB6 OME displayed a similar global gene expression profile to NOK-based OME with increased expression of many common pro-inflammatory molecules such as chemokines (CXCL8), cytokines (IL-6) and adhesion molecules (ICAM-1) when analysed by gene array and qPCR. Similarly, pathway analysis showed that both FNB6 and NOK models initiated similar intracellular signalling upon stimulation. Gene expression in FNB6 OME was more consistent than NOK-based OME that suffered from donor variation in response to stimuli. Mucosal equivalents based on immortalised FNB6 cells are accessible, reproducible and will provide an alternative animal experimental system for studying mucosal drug delivery systems, host-pathogen interactions and drug-induced toxicity.

Keywords:

Oral mucosa, oral keratinocytes, mucosal model, cytokine, immune response

Introduction

The use of three-dimensional models of human tissue has come to the forefront of medical research in recent years and has shown to be a powerful tool in both industry and academia for the testing of drug responses and tissue toxicity (1). Physiologically relevant 3D models are rapidly becoming the preferred experimental *in vitro* model because cells cultured as monolayers do not represent the complex tissue microenvironment present in living organisms and often prove to be poor predictors drug-induced cell toxicity (2, 3). Moreover, the desire to replace, refine or reduce animals in experimental procedures where possible has prompted a move away from *in vivo* research to *in vitro* assays in many areas of science. This is especially true for epithelial biology in response to the Organisation for Economic Co-operation and Development (OECD) guidelines and European Commission regulation (440/2008/EC) unequivocally promoting the use of validated, tissue engineered *in vitro* human epidermal models as alternative models for skin/eye irritation (No.439), sensitisation (No.442D) and corrosion tests (No.431; OECD (2013)). Oral mucosal equivalents (OME) are also being increasingly used in a wider range of scientific research including host-pathogen interactions (4, 5), xenobiotic enzyme metabolism (6, 7), cancer biology (8, 9) and biomaterial compatibility (10, 11). Currently, most OME are based on the co-culture of primary normal oral keratinocytes (NOK) on top of a hydrogel matrix containing normal oral fibroblast (NOF) cultured at an air-to-liquid interface (12, 13). However, in some instances OME based on the use of malignant keratinocytes to replace NOK have been used to model the oral mucosa (14, 15). The paracrine interactions between the NOF and NOK are essential for the growth and differentiation of the keratinocytes to produce a multilayer, stratified squamous epithelium (16). Although the physiological and histological structure of the oral mucosa is very similar to that of the skin, there are key differences. Similar to skin the oral

epithelium is comprised of basal cells that are attached to the connective tissue basement membrane via hemidesmosome contacts. As the basal cells divide and migrate apically into the suprabasal spinous layer they undergo continuous alterations in gene expression and morphology that eventually differentiate into cells that make up the granular layer, which constitutes the main permeability barrier of the epithelium. In some anatomical parts of the oral mucosa such as the hard palate, these cells then differentiate further into a highly keratinised, cornified layer similar to the skin, but in other areas such as the buccal mucosa or lingual regions the mucosa is non-keratinised. The basal cells express keratin 5/14 whilst, in contrast to the skin, the suprabasal cells express keratin 4/13 in addition to late epidermal differentiation proteins involucrin and flaggarin. OME based on primary cells have shown that these models express all of the structural and histological characteristics as normal tissue and are excellent substitute models for native tissue (8, 17, 18). However, there are several disadvantages with constructing OME using primary keratinocytes. These include the dependency on the supply of isolated keratinocytes from surgically extracted donor oral tissue, the inherent donor-to-donor variation from one batch of keratinocytes to another and the restricted proliferation capacity of these cells. To compound these issues and in contrast to skin keratinocytes, the commercial supply of oral keratinocytes is severely restricted. Therefore, there is a need to generate OME based on immortalised keratinocytes to enable more widespread access to OME and to reduce donor variation. Normal oral keratinocytes have been immortalized by over-expression of hTERT using stable transfection (13), the consequence of which prevents telomere shortening thereby increasing the life-span and proliferative capacity of cells whilst maintaining their phenotype (19).

In this study we examined whether FNB6 TERT-immortalised oral keratinocytes are a suitable cellular source to construct a fully differentiated stratified squamous epithelium

that is phenotypically and histologically similar to normal oral mucosa and OME based on NOK. In addition, the innate immune functionality of the epithelium was tested against NOK-based models based on their gene and protein expression responses to pro-inflammatory cytokines and bacterial lipopolysaccharide to mimic oral inflammation.

Materials and methods

Cell culture of primary cells, immortalized oral keratinocytes and oral cancer cells

FNB6-TERT immortalised oral keratinocytes (Beatson Institute for Cancer Research, Glasgow, UK; commercially available at Ximbia, London, UK) originally isolated from the buccal mucosa (20) and H357, an oral squamous cell carcinoma cell line derived from the tongue (21) (Health Protection Agency Culture Collections, Salisbury, UK) were cultured in Green's Medium consisting of Dulbecco's Modified Eagle's Medium (DMEM) and Ham's F12 medium in a 3:1 (v/v) ratio supplemented with 10% (v/v) foetal calf serum (FCS), 0.1 µM cholera toxin, 10 ng/ml epidermal growth factor, 0.4 µg/ml hydrocortisone, 0.18 mM adenine, 5 µg/ml insulin, 5 µg/ml transferrin, 2 mM glutamine, 0.2 µM triiodothyronine, 0.625 µg/ml amphotericin B, 100 IU/ml penicillin and 100 µg/ml streptomycin. Normal oral fibroblasts were isolated from the connective tissue of biopsies obtained from the gingival oral mucosa from patients during routine dental procedures with written, informed consent (ethical approval number 09/H1308/66) as previously described (8) and cultured in DMEM supplemented with 10% FCS, 2 mM glutamine, 100 IU/ml penicillin and 100 µg/ml streptomycin.

Oral mucosal equivalent

Oral mucosal models were constructed as previously described (22). Briefly, freeze dried rat-tail collagen was dissolved in 0.1 M acetic acid to give a final concentration of 5 mg/ml and stored at 4°C until use. FBS, 10 x DMEM, L-Glutamine and reconstitution buffer (2.2% sodium bicarbonate, 4.8% HEPES, 0.248% NaOH in dH₂O) were added to the collagen and pH adjusted to 7.4. Gingival NOF were added to the collagen mixture at a concentration of 2.5 x 10⁵ cells/ml before adding 1 ml to 12 mm cell culture transwell inserts (0.4 µm pore, Millipore) and allowed to set in a humidified atmosphere at 37°C for 2 h. Inserts were submerged in media and incubated for 2 d, after which 5 x 10⁵ oral keratinocytes (H357 or FNB6) per model were seeded on to the surface. After a further 2 d, the models were raised to an air-to-liquid interface and cultured for 14 d. ORL-300-FT full-thickness OME based on buccal-derived NOK cultured on top of a gingival fibroblast-populated collagen hydrogel scaffold were purchased from MatTek Corp., (Ashland, MA, USA) and used according to the manufactures instructions.

Stimulation of OME

OME were stimulated by placing 50 µl of 20 ng/ml TNFα + 10 ng/ml IL-1β or 100 ng/ml LPS (*E. coli* serotype O55:B5, Sigma, Poole, UK) on top of the models and incubating for 6 or 24 h in a humidified atmosphere at 37°C. Unstimulated controls consisted of OME incubated with medium alone.

Histological analysis

For histological analysis, OME were removed from the culture medium, washed with PBS and fixed in 10% buffered formalin overnight. The entire model (connective tissue and epithelium) were removed from the transwell insert along with the polycarbonate filter and

subjected to routine histological processing and then paraffin wax embedded. Five µm sections were cut using a Leica RM2235 microtome (Leica microsystems) and stained with Haematoxylin and eosin (H&E) or subject to immunohistochemistry (IHC). Formalin fixed paraffin embedded normal oral mucosal tissue was used as a control for histological and immunohistochemical analysis, ethical approval was granted by the Sheffield Research Ethics Committee (Ref: 07/H1309/105).

Immunohistochemical analysis

Sections were dewaxed, rehydrated through a series of alcohol dilutions and endogenous peroxidase neutralised with 3% hydrogen peroxide in methanol for 20 minutes. Antigen retrieval was achieved using 0.01 M Tri sodium citrate buffer (pH 6) at high temperature. Following blocking with normal goat serum for 20 minutes at room temperature sections were incubated with primary antibody (Table 1) or IgG isotype control antibody for 1 h at room temperature. Secondary antibody and avidin-biotin complex (ABC) provided with Vectastain Elite ABC kit (Vector labs, Peterborough, UK) were used in accordance with the manufacturer's instructions. Finally, 3'-diaminobenzidine tetrahydrochloride (DAB; Vector labs, Peterborough, UK) was used to visualise peroxidase activity and the sections counterstained with haematoxylin, dehydrated and mounted in DPX. Light microscope images were taken using an Olympus BX51 microscope and Colour view IIIu camera with associated Cell^D software (Olympus soft imaging solutions, GmbH, Münster, Germany).

Lactate Dehydrogenase (LDH) release assay

Cell damage was analysed by measuring the release of LDH into the culture medium using a CytoTox96 enzyme assay kit as described in the manufacturer's instructions (Promega,

Southampton, UK). Briefly, 50 µl of conditioned culture medium from cell cultures was added to 50 µl of reconstituted substrate mix in a well of a 96-well flat-bottomed plate. The plate was incubated for 30 minutes at room temperature before stopping the reaction using 50 µl acetic acid and the absorbance measured at 492 nm.

Quantitative Real-Time PCR (qRT-PCR)

Total RNA was extracted from cells using Isolate II RNA kit (Bioline, London, UK). 500 ng of total RNA was reverse transcribed using High Capacity RNA to cDNA kit (Life Technologies, Paisley, UK) cDNA (0.5 µl) was amplified with 5 µl 2X TaqMan gene expression master mix, 0.5 µl Taq-Man pre-designed gene probes and 3.5 µl nuclease-free water, using an Applied Biosystems Real-Time PCR System. The human TaqMan gene expression probes used were CXCL8 (hs00174103_m1) and Intercellular adhesion molecule-1 (ICAM-1) (hs00164932_m1). β-2-microglobulin (hs00187842_m1) was used as the reference control gene (all Applied Biosystems). Real-time PCR cycles were: 95°C for 10 minutes followed by 40 cycles of 15 seconds at 95°C followed by 1 minute at 60°C. Real-Time PCR were analysed in 3 independent experiments. The threshold cycle (Ct) was normalised against the reference gene (ΔCt) and then fold changes in expression relative to untreated groups calculated using the formula $2^{-\Delta\Delta Ct}$.

Enzyme-linked immunosorbent assay

Commercially available ELISA (OptEIA™, BD Bioscience) kits were used according to the manufacturer's instructions to measure levels of CXCL8 and IL-6 in tissue culture conditioned medium of OME as described previously (4).

Gene Array

Linear amplification of RNA was performed using GeneChip® 3' IVT Express Kit (Affymetrix, Santa Clara, CA, USA) following the manufacturer's instructions. Briefly, 200 ng mRNA was reverse transcribed using an oligo(dT) primer and then converted to double-stranded cDNA containing a T7 polymerase promoter site. Antisense RNA containing biotinylated dUTPs was generated by T7 promoter-driven linear amplification for 16 hours at 40°C. 15 µg of the antisense RNA was fragmented in Fragmentation Buffer at 94°C for 30 minutes. One µl of fragmented antisense RNA was assessed using an RNA 6000 Nano Chip on a 2100 Bioanalyzer (Agilent Technologies, Santa Clara, CA). Hybridisation was carried out following using the instructions in the GeneChip® Hybridization, Wash, and Stain Kit (Affymetrix, Santa Clara, CA). Briefly 12.5 µg of fragmented antisense RNA was included in a cocktail that also contained serial concentrations of pre-labelled hybridization controls (bioB, bioC, bioD, and cre genes) and positive oligonucleotide B2 control (B2 oligo). After 16 hours hybridisation at 42°C with rotation at 60 rpm, the GeneChips were washed and stained in a GeneChip Fluidics Station 450 (Affymetrix) following the protocol EukGE-WS2v5_450 as described in the manufacturer's manual, and scanning was performed using a GeneChip Scanner 3000 7G (Affymetrix). Following scanning, image files (.CEL) were processed using the Expression Console Software (Affymetrix) in order to carry our quality control and to prepare an RMA normalised dataset of the signal intensity for each probe set. Differential gene expression was determined using the Qlucore 'omics Explorer Package (Qlucore, Lund, Sweden).

Statistics

Data are presented as mean values ± standard deviation (SD) of three independent experiments (n=3) with each test performed in triplicate unless otherwise stated. ANOVA

multiple statistical comparisons were performed using GraphPad Prism v6.00 (GraphPad Software, La Jolla, CA, USA) and differences between test and control groups were considered significant when $p < 0.05$.

Results

OME constructed of human FNB6 TERT-immortalised oral keratinocytes resembles native skin and NOK-based OME.

Full-thickness, tissue-engineered oral mucosa was generated using either immortalised buccal keratinocytes (FNB6) or the OSCC cell line (H357) and the morphology, differentiation and proliferation status of these models compared to commercially available NOK-based OME or healthy, normal oral mucosa. Histological analysis showed that OME generated using FNB6 immortalised oral keratinocytes produced a multi-layered well-defined, stratified epithelium approximately 120 µm in thickness with ki-67 positive proliferating cells restricted to the basal keratinocytes (Fig. 1 A&B). The epithelium of FNB6-based OME was stratified, non-keratinised and differentiated with the stratum spinosum and stratum granulosum layers immune-positive for cytokeratin 13. In addition, these OME displayed immuno-reactive staining for E-cadherin showing the presence of well-defined cell-to-cell contacts (Fig. 1 C-E). The histology and expression of these markers was generally comparable to those seen in both the NOK-based OME and particularly the normal buccal mucosa (Fig. 1 A-E). Interestingly, both FNB6 OME and NOK-based OME displayed cytokeratin 14 expression throughout the entire epithelium whereas in normal oral mucosa this was mainly restricted to the basal epithelial cells. In stark contrast, OME generated using the OSCC cell line H357 produced a multi-layered but non-stratified epithelium with ki67-positive proliferating cells throughout the stratum spinosum and stratum granulosum, and not restricted to the basal layer (Fig. 1). Although E-cadherin staining was positive and extensive confirming cell-to-cell contacts, cytokeratin 13 and 14 expression was abnormal with immune-positive staining observed throughout the epithelium showing aberrant of

keratinocyte differentiation. Desquamation of Keratinocytes from the surface of the epithelium was observed for both NOK and FNB6 OME but not for H357 models. Furthermore, in contrast to models based on NOK and FNB6 cells, H357 mucosal models displayed frequent evidence of epithelial invasion into the underlying collagen scaffold (Fig. 1).

FNB6 TERT-immortalised OME is functionally responsive to pro-inflammatory cytokine stimulation.

Previously, we have shown that OME can be used to study gene and cytokine responses in response to cytokine and microbial insult (14, 22). To investigate the innate immune response of the OME epithelium, FNB6, H357 and NOK-based OME were treated with a combination of TNF α and IL-1 β or LPS and the epithelium RNA and conditioned medium generated from the entire OME was analysed for chemokine (CXCL8) and adhesion molecule (ICAM-1) gene expression and cytokine secretion (CXCL8, IL6) respectively. Treatment with cytokines or LPS had no effect on the morphology of any of the OME nor did these inflammatory mediators cause any statistically significant difference in release of LDH compared to un-stimulated controls (data not shown). Treatment with TNF α + IL-1 β caused a statistically significant increase ($p<0.05$) in the gene expression of CXCL8 (10-fold) and ICAM-1 (4-fold) in FNB6 OME compared to controls (Fig. 2A & B) and this trend was mirrored in both NOK-based and H357 OME where gene expression of CXCL8 was increased 4-fold for both NOK and H357 OME and 10-fold for ICAM-1 (NOK OME) and 4-fold for H357 OME, respectively, compared to unstimulated controls in all cases; Fig. 2A-F). Stimulation with LPS did not statistically significantly ($p>0.5$) increase the gene expression of CXCL8 or ICAM-1 in any of the OME although expression of CXCL8 was consistently raised in NOK-

based OME compared to controls (Fig. 2A-F). In addition, pro-inflammatory cytokine stimulation resulted in a statistically significant ($p<0.05$) increase in CXCL8 secretion in FNB6 and H357 OME, with these showing a 6-fold increase in concentration compared to untreated controls (Fig. 3). FNB6 OME showed no statistically significant ($p>0.05$) increase in CXCL8 secretion in response to LPS compared to control, whereas H357 models showed a 5-fold increase in CXCL8 secretion compared to untreated controls (Fig 3.). Surprisingly, NOK OME showed no statistically significant increase in secreted CXCL8 in response to LPS or TNF α and IL-1 β treatment (Fig. 3).

FNB6 TERT-immortalised OME has a similar pro-inflammatory gene profile to NOK-based OME.

Since FNB6 OME were structurally and histologically similar to NOK OME and that both OME responded to cytokine stimulation by release of CXCL8 and ICAM-1, we wanted to determine if this similarity in epithelial gene expression was extended at a global scale. Therefore, gene expression of cytokine or LPS stimulated FNB6 and NOK epithelium were subjected to microarray analysis and compared to unstimulated controls. Hierarchical gene cluster analysis showed that gene expression in unstimulated cells was similar for NOK and FNB6 models with OME producing a similar global gene expression profile (Fig. 4A). Moreover, at a global scale both NOK-based and FNB6 OME displayed similar gene profiles when stimulated with cytokines with responses being indistinguishable on hierarchical analysis between the two models (Fig. 4A). In contrast, the global pattern of gene expression of the two models in response to LPS stimulation was un-clustered showing desperate patterns between models (Fig. 4A).

Additional principal component analyses confirmed these finding and showed that the overall gene responses of FNB6 and NOK OME clustered together when these models were unstimulated or stimulated with cytokines, LPS or (Fig. 4B). The top 10 up-regulated genes for cytokine stimulated FNB6 and NOK OME are shown in Tables 2 & 3. Overall, the genes up-regulated by cytokine treatment in both FNB6 and NOK OME are pro-inflammatory in nature and include IL-6, pentraxin-related protein-3 (PTX3), prostaglandin-endoperoxide synthase-2 (PTGS2), Tumor Necrosis Factor-inducible gene 6 protein (TNFA1P6) and an array chemokines. Moreover, signal transduction pathway data analysis from the gene data of both FNB6 and NOK OME show that activation of the NF κ B signaling pathway is common to both cytokine treated OME with key regulatory factors such as IKK γ , I κ B α being affected. In addition, other pro-inflammatory pathways were commonly activated such as MAPK, JNK and MEK1/2 (Fig. 5A). The mean global expression data was then broken down into expression data from each individual experiment to examine the inter-experimental variability between different batches of OME and to determine if NOK models are subjected to donor variability. Figure 5B shows that OME generated from FNB6 models cluster together suggesting a similar global gene response pattern between experiments and provide evidence of good inter-experimental variability. In contrast, the global expression gene expression profiles of NOK OME were statistically significantly ($p<0.05$) different with one NOK OME showing a distinct cluster pattern compared to the other NOK OME (Fig. 5B).

Discussion

Advances in tissue culture technology and the commercial availability of NOK-based OME has led to a dramatic increase in their use both in industry and academia, and it is now generally accepted that use of 3D tissue models provides more robust data compared to 2D counterpart (23). However, there are drawbacks and the lack of availability and inherent donor-to-donor variability of oral keratinocytes, and the financial cost of purchasing commercially available OME have hindered the universal use of these model systems. To circumvent these issues some investigators have turned to using OME based on oral cancer cells to mimic the oral mucosa (14). Previous studies have employed TERT-immortalised oral keratinocytes (OKF6) (13) in OME but these models have not been characterised thoroughly and in some studies have resulted in poorly differentiated epithelium or epithelial layers of only 3-4 cells thick (24, 25). In this study we investigated whether FNB6 TERT-immortalised oral keratinocytes could be used to replace NOK in OME and whether their gene expression responses were similar to NOK OME upon stimulation with pro-inflammatory stimuli.

The histological structure and expression of key markers of epithelial integrity, stratification, differentiation and keratinisation were similar between the normal oral mucosa and OME generated from NOK and FNB6 cells. Similar findings were observed in a recent study examining the histological similarities of 3D equivalent models based on TERT-immortalised gingival keratinocytes when compared to gingival tissue (26). However, there are key differences between these oral equivalent models the most important of which is the presence of a non-keratinised epithelium in FNB6 models compared to those based on immortalised gingival keratinocytes that are keratinised. Therefore, models based on TERT-immortalised oral keratinocytes have the ability to retain their distinct keratinisation status

(non-keratinised, buccal for FNB6 and keratinised gingiva for immortalised gingival keratinocytes) and display a similar respective keratinisation phenotype to OME based on normal buccal or gingival keratinocytes despite all these models containing gingival fibroblasts in the connective tissue scaffold. OME created using the oral squamous cell carcinoma cell line H357 exhibited characteristics more consistent with the origin of these cells with proliferation in all levels of the epithelium, a lack of stratification and abnormal expression of differentiation markers. At times invasion of the underlying collagen matrix was observed; a characteristic that makes such 3D models more amenable to the study of tumorigenesis than normal mucosal physiology (8, 27).

The human oral cavity harbours a range of micro-organisms that is continuously evolving and responding to environmental conditions. The interaction between these organisms and the host's immune system is carefully regulated to prevent the development of disease pathology. The epithelium is the first line of defence against bacteria both physically and in triggering the immune response (28, 29). Oral keratinocytes and fibroblasts co-ordinate the initial innate immune response through the production of cytokines and chemokines that attract immune cells to the site of infection (28, 30). Previous reports suggest that fibroblasts play an important role in the epithelial inflammatory response (31). However, a minimal response to oral bacteria was noted in NOK OME compared to primary epithelial cell monolayers which the authors suggested was due to poor penetration of bacteria into the epithelial layer in a way that presumably soluble mediators circumvent (32). Furthermore, there is little change in cytokine production by 3D models exposed to *P. gingivalis* with and without fibroblasts (14).

We have shown that NOK-based and FNB6 OME respond to the pro-inflammatory stimulus of IL-1 β and TNF α in a similar way and that this can consistently be monitored using CXCL8 ELISA on the conditioned medium, CXCL8 and ICAM-1 qPCR and broader screening using gene array analysis. Others have shown that 3D models containing multiple cell types relevant to intestine respond to IL-1 by releasing CXCL8 and that anti-inflammatory interventions can be tested using such a model (33). Skin equivalents using immortalised keratinocytes have also been shown to respond to thermal injury by enhanced secretion of inflammatory cytokines including IL-6 and CXCL8, although generally the level of this response was less than models using primary keratinocytes (34).

The response to *E.coli* LPS was much less obvious for all models than that initiated by cytokine stimulus. Others have reported a poor response of oral epithelial cells to LPS (35) that may relate to lack of expression of the relevant TLRs, CD14 or the culture conditions. TLR4 expression has been previously observed on NOK and immortalised oral keratinocytes by immunohistochemistry and PCR (36, 37). TLR4 expression was donor dependent for NOK and may explain the variation in gene expression observed in our whole genome transcription analysis in response to LPS stimulation between immortalised FNB6 and NOK. In addition, we found that OME comprised of oral cancer cells displayed increased CXCL8 expression in response to LPS compared to OME comprised of NOK or immortalised oral keratinocytes that may be due to increased expression of TLR4 observed on OSCC cells compared to normal oral mucosa (38). It may be that by using whole bacteria or the LPS from oral species that a more appropriate response would be elicited. Sugiyama et al (2002) demonstrated that monolayers of gingival epithelial cells responded to surface components of *Porphyromonas gingivalis* and *Prevotella intermedia* by increasing production of CXCL8,

GCSF, GMCSF and ICAM-1 but that LPS from *P. intermedia* or *E. coli* did not (39). Others showed that live *Streptococcus salivarius* is capable of inducing IL-6, CXCL8 and TNF α in an oral mucosal model (40). More recently it has been suggested that the more complex nature of polymicrobial diseases such as periodontal disease may be better reflected by challenging oral mucosal models with multi-species biofilms (41, 42). Some cytokine responses in OME using oral cells have been significant (41) whilst others have been more modest (43, 44) and 3D oral mucosal models generated using SV40 T-antigen transformed gingival epithelial cells responded to *Aggregatibacter actinomycetemcomitans* LPS and that this effect is enhanced by the presence of fibroblasts (44).

Array analysis revealed a similar inflammatory gene signature pathway for both NOK and FNB6 OME in response to the cytokines with more genes significantly up-regulated than down-regulated. Of the top 10 genes overexpressed between NOK and FNB6 OME most were predominately associated with leukocyte chemotaxis that would mediate inflammatory cell recruitment into the epithelium (CXCL5, CCL20, CXCL8, CXCL3). Pathway analysis revealed that common downstream mediators such as NFkB, which are known targets of IL-1 β and TNF α , are influenced in a similar way between NOK and FNB6 models confirming that this is a suitable stimulus to produce a model of inflamed oral mucosa (45). What was apparent however was that different batches of NOK OME that showed variation in their response. The response of FNB6-based OME was more consistent from batch to batch and as such a viable model of inflamed oral mucosa.

In conclusion, this study shows that OME based on immortalised FNB6 cells are able to mimic the native oral mucosa structure and replicate tissue responses to inflammatory

mediators observed with NOK-based models and therefore provide a readily available alternative to NOK.

Acknowledgements

The authors thank Dr Paul Health (University of Sheffield) for performing the gene array and helping with the data analysis, and Ms Brenka McCabe for technical help with qPCR.

Author Disclosure Statement

JO, FP, JM and HMT are employees of Colgate-Palmolive Company which provided financial support for the project. LJ, CM, HC and SW have no conflict of interest.

References

1. Peck, Y., and Wang, D.A. Three-dimensionally engineered biomimetic tissue models for *in vitro* drug evaluation: delivery, efficacy and toxicity. *Expert Opin Drug Deliv* **10**, 369, 2013.
2. Cukierman, E., Pankov, R., Stevens, D.R., and Yamada, K.M. Taking cell-matrix adhesions to the third dimension. *Science* **294**, 1708, 2001.
3. Xu, X., Farach-Carson, M.C., and Jia, X. Three-dimensional *in vitro* tumor models for cancer research and drug evaluation. *Biotechnol Adv* **32**, 1256, 2014.
4. Yadav, N.R., Murdoch, C., Saville, S.P., and Thornhill, M.H. Evaluation of tissue engineered models of the oral mucosa to investigate oral candidiasis. *Microbial Pathogenesis* **50**, 278, 2011.
5. Belibasakis, G.N., Thurnheer, T., and Bostanci, N. Interleukin-8 responses of multi-layer gingival epithelia to subgingival biofilms: role of the "red complex" species. *PLoS One* **8**, e81581, 2013.
6. Kim, J.W., Ho, W.J., and Wu, B.M. The role of the 3D environment in hypoxia-induced drug and apoptosis resistance. *Anticancer Res* **31**, 3237, 2011.
7. Gotz, C., Pfeiffer, R., Tigges, J., Ruwiedel, K., Hubenthal, U., Merk, H.F., Krutmann, J., Edwards, R.J., Abel, J., Pease, C., Goebel, C., Hewitt, N., and Fritzsche, E. Xenobiotic metabolism capacities of human skin in comparison with a 3D-epidermis model and keratinocyte-based cell culture as *in vitro* alternatives for chemical testing: phase II enzymes. *Exp Dermatol* **21**, 364, 2012.
8. Colley, H.E., Hearnden, V., Jones, A.V., Weinreb, P.H., Violette, S.M., Macneil, S., Thornhill, M.H., and Murdoch, C. Development of tissue-engineered models of oral dysplasia and early invasive oral squamous cell carcinoma. *Br J Cancer* **105**, 1582, 2011.

9. Sapkota, D., Bruland, O., Parajuli, H., Osman, T.A., Teh, M.T., Johannessen, A.C., and Costea, D.E. S100A16 promotes differentiation and contributes to a less aggressive tumor phenotype in oral squamous cell carcinoma. *BMC Cancer* **15**, 631, 2015.
10. Chai, W.L., Brook, I.M., Palmquist, A., van Noort, R., and Moharamzadeh, K. The biological seal of the implant-soft tissue interface evaluated in a tissue-engineered oral mucosal model. *J R Soc Interface* **9**, 3528, 2012.
11. Moharamzadeh, K., Brook, I.M., Van Noort, R., Scutt, A.M., Smith, K.G., and Thornhill, M.H. Development, optimization and characterization of a full-thickness tissue engineered human oral mucosal model for biological assessment of dental biomaterials. *J Mat Sci-Mat Med* **19**, 1793, 2008.
12. Moharamzadeh, K., Colley, H., Murdoch, C., Hearnden, V., Chai, W.L., Brook, I.M., Thornhill, M.H., and Macneil, S. Tissue-engineered oral mucosa. *J Dent Res* **91**, 642, 2012.
13. Dongari-Bagtzoglou, A., and Kashleva, H. Development of a highly reproducible three-dimensional organotypic model of the oral mucosa. *Nature Protocols* **1**, 2012, 2006.
14. Pinnock, A., Murdoch, C., Moharamzadeh, K., Whawell, S., and Douglas, C.W. Characterisation and optimisation of organotypic oral mucosal models to study *Porphyromonas gingivalis* invasion. *Microbes Infect* **16**, 310, 2014.
15. Schaller, M., Boeld, U., Oberbauer, S., Hamm, G., Hube, B., and Korting, H.C. Polymorphonuclear leukocytes (PMNs) induce protective Th1-type cytokine epithelial responses in an in vitro model of oral candidosis. *Microbiol* **150**, 2807, 2004.
16. Costea, D.E., Loro, L.L., Dimba, E.A., Vintermyr, O.K., and Johannessen, A.C. Crucial effects of fibroblasts and keratinocyte growth factor on morphogenesis of reconstituted human oral epithelium. *J Invest Dermatol* **121**, 1479, 2003.

17. Tra, W.M., van Neck, J.W., Hovius, S.E., van Osch, G.J., and Perez-Amodio, S. Characterization of a three-dimensional mucosal equivalent: similarities and differences with native oral mucosa. *Cells, Tissues, Organs* **195**, 185, 2012.
18. Rouabchia, M., and Deslauriers, N. Production and characterization of an in vitro engineered human oral mucosa. *Biochem Cell Biol* **80**, 189, 2002.
19. Lee, K.M., Choi, K.H., and Ouellette, M.M. Use of exogenous hTERT to immortalize primary human cells. *Cytotechnol* **45**, 33, 2004.
20. McGregor, F., Muntoni, A., Fleming, J., Brown, J., Felix, D.H., MacDonald, D.G., Parkinson, E.K., and Harrison, P.R. Molecular changes associated with oral dysplasia progression and acquisition of immortality: Potential for its reversal by 5-azacytidine. *Cancer Res* **62**, 4757, 2002.
21. Yeudall, W.A., Torrance, L.K., Elsegood, K.A., Speight, P., Scully, C., and Prime, S.S. Ras Gene Point Mutation Is a Rare Event in Premalignant Tissues and Malignant-Cells and Tissues from Oral Mucosal Lesions. *Oral Oncol* **29B**, 63, 1993.
22. Wayakanon, K., Thornhill, M.H., Douglas, C.W.I., Lewis, A.L., Warren, N.J., Pinnock, A., Armes, S.P., Battaglia, G., and Murdoch, C. Polymersome-mediated intracellular delivery of antibiotics to treat *Porphyromonas gingivalis*-infected oral epithelial cells. *Faseb Journal* **27**, 4455, 2013.
23. Rouwkema, J., Gibbs, S., Lutolf, M.P., Martin, I., Vunjak-Novakovic, G., and Malda, J. In vitro platforms for tissue engineering: implications for basic research and clinical translation. *J Tissue Eng Regen Med* **5**, e164, 2011.
24. Almela, T., Brook, I.M., and Moharamzadeh, K. Development of three-dimensional tissue engineered bone-oral mucosal composite models. *J Mat Sci-Mat Med* **27** 2016.

25. McLeod, N.M.H., Moutasim, K.A., Brennan, P.A., Thomas, G., and Jenei, V. In Vitro Effect of Bisphosphonates on Oral Keratinocytes and Fibroblasts. *J Oral Maxillofac Surg* **72**, 503, 2014.
26. Buskermolen, J.K., Reijnders, C.M., Spiekstra, S.W., Steinberg, T., Kleverlaan, C.J., Feilzer, A.J., Bakker, A.D., and Gibbs, S. Development of a Full Thickness Human Gingiva Equivalent Constructed from Immortalized Keratinocytes and Fibroblasts. *Tissue Eng Part C Methods* 2016.
27. Nystrom, M.L., Thomas, G.L., Stone, M., Mackenzie, I.C., Hart, I.R., and Marshall, J.F. Development of a quantitative method to analyse tumour cell invasion in organotypic culture. *J Pathol* **205**, 468, 2005.
28. Fukui, A., Ohta, K., Nishi, H., Shigeishi, H., Tobiume, K., Takechi, M., and Kamata, N. Interleukin-8 and CXCL10 expression in oral keratinocytes and fibroblasts via Toll-like receptors. *Microbiol Immunol* **57**, 198, 2013.
29. Yumoto, H., Nakae, H., Fujinaka, K., Ebisu, S., and Matsuo, T. Interleukin-6 (IL-6) and IL-8 are induced in human oral epithelial cells in response to exposure to periodontopathic *Eikenella corrodens*. *Infect Immun* **67**, 384, 1999.
30. Akira, S. Toll-like receptor signaling. *J Biol Chem* **278**, 38105, 2003.
31. Boxman, I.L., Ruwhof, C., Boerman, O.C., Lowik, C.W., and Ponec, M. Role of fibroblasts in the regulation of proinflammatory interleukin IL-1, IL-6 and IL-8 levels induced by keratinocyte-derived IL-1. *Arch Dermatol Res* **288**, 391, 1996.
32. Kimball, J.R., Nittayananta, W., Klausner, M., Chung, W.O., and Dale, B.A. Antimicrobial barrier of an in vitro oral epithelia model. *Arch Oral Biol* **51**, 775, 2006.

33. Leonard, F., Ali, H., Collnot, E.M., Crielaard, B.J., Lammers, T., Storm, G., and Lehr, C.M. Screening of Budesonide Nanoformulations for Treatment of Inflammatory Bowel Disease in an Inflamed 3D Cell-Culture Model. *ALTEX* **29**, 275, 2012.
34. Reijnders, C.M.A., van Lier, A., Roffel, S., Kramer, D., Schepers, R.J., and Gibbs, S. Development of a Full-Thickness Human Skin Equivalent In Vitro Model Derived from TERT-Immortalized Keratinocytes and Fibroblasts. *Tissue Eng Part A* **21**, 2448, 2015.
35. Uehara, A., Sugawara, S., Tamai, R., and Takada, H. Contrasting responses of human gingival and colonic epithelial cells to lipopolysaccharides, lipoteichoic acids and peptidoglycans in the presence of soluble CD14. *Med Microbiol Immunol* **189**, 185, 2001.
36. Sugawara, Y., Uehara, A., Fujimoto, Y., Kusumoto, S., Fukase, K., Shibata, K., Sugawara, S., Sasano, T., and Takada, H. Toll-like receptors, NOD1, and NOD2 in oral epithelial cells. *J Dent Res* **85**, 524, 2006.
37. Beklen, A., Hukkanen, M., Richardson, R., and Konttinen, Y.T. Immunohistochemical localization of Toll-like receptors 1-10 in periodontitis. *Oral Microbiol Immunol* **23**, 425, 2008.
38. Kotrashetti, V.S., Nayak, R., Bhat, K., Hosmani, J., and Somannavar, P. Immunohistochemical expression of TLR4 and TLR9 in various grades of oral epithelial dysplasia and squamous cell carcinoma, and their roles in tumor progression: a pilot study. *Biotechnic Histochem* **88**, 311, 2013.
39. Sugiyama, A., Uehara, A., Iki, K., Matsushita, K., Nakamura, R., Ogawa, T., Sugawara, S., and Takada, H. Activation of human gingival epithelial cells by cell-surface components of black-pigmented bacteria: augmentation of production of interleukin-8, granulocyte colony-stimulating factor and granulocyte-macrophage colony-stimulating factor and expression of intercellular adhesion molecule 1. *J Med Microbiol* **51**, 27, 2002.

40. Mostefaoui, Y., Bart, C., Frenette, M., and Rouabchia, M. *Candida albicans* and *Streptococcus salivarius* modulate IL-6, IL-8, and TNF-alpha expression and secretion by engineered human oral mucosa cells. *Cell Microbiol* **6**, 1085, 2004.
41. Millhouse, E., Jose, A., Sherry, L., Lappin, D.F., Patel, N., Middleton, A.M., Pratten, J., Culshaw, S., and Ramage, G. Development of an in vitro periodontal biofilm model for assessing antimicrobial and host modulatory effects of bioactive molecules. *BMC Oral Health* **14**2014.
42. Belibasakis, G.N., Kast, J.I., Thurnheer, T., Akdis, C.A., and Bostanci, N. The expression of gingival epithelial junctions in response to subgingival biofilms. *Virulence* **6**, 704, 2015.
43. Bao, K., Papadimitropoulos, A., Akgul, B., Belibasakis, G.N., and Bostanci, N. Establishment of an oral infection model resembling the periodontal pocket in a perfusion bioreactor system. *Virulence* **6**, 265, 2015.
44. Bedran, T.B.L., Mayer, M.P.A., Spolidorio, D.P., and Grenier, D. Synergistic Anti-Inflammatory Activity of the Antimicrobial Peptides Human Beta-Defensin-3 (hBD-3) and Cathelicidin (LL-37) in a Three-Dimensional Co-Culture Model of Gingival Epithelial Cells and Fibroblasts. *PloS One* **9**2014.
45. Akira, S., and Takeda, K. Toll-like receptor signalling. *Nat Rev Immunol* **4**, 499, 2004.

Table 1. Details of antibodies used for immunohistochemistry.

Table 2. Top 10 genes up-regulated by NOK-OME upon stimulation with TNF- α and IL-1 β .

Table 3. Top 10 genes up-regulated by FNB6-OME upon stimulation with TNF- α and IL-1 β .

Gene	Fold-Change	p-value
IL6	7.99	0.0011
CXCL8	7.11	0.0001
PTX3	5.87	0.0125
PTGS2	4.86	0.0295
CXCL3	4.75	0.0177
CCL20	4.65	0.0090
CXCL5	4.23	0.0007
IRAK2	3.81	0.0177
IL36G	3.81	0.0254
TNFAIP3	3.58	0.0153

Table 3. Top 10 genes up-regulated by FNB6-OME upon stimulation with TNF- α and IL-1 β .**Figure legends**

Tissue Engineering Part C: Methods
 Development and characterisation of in vitro human oral mucosal equivalents derived from immortalised oral keratinocytes (doi: 10.1089/ten.TEC.2016.0310)
 This article has been peer-reviewed and accepted for publication, but has yet to undergo final editing and proof correction. The final published version may differ from this proof.
 Development and characterisation of in vitro human oral mucosal equivalents derived from immortalised oral keratinocytes (doi: 10.1089/ten.TEC.2016.0310)
 This paper has been peer-reviewed and accepted for publication, but has yet to undergo copyediting and proof correction. The final published version may differ from this proof.

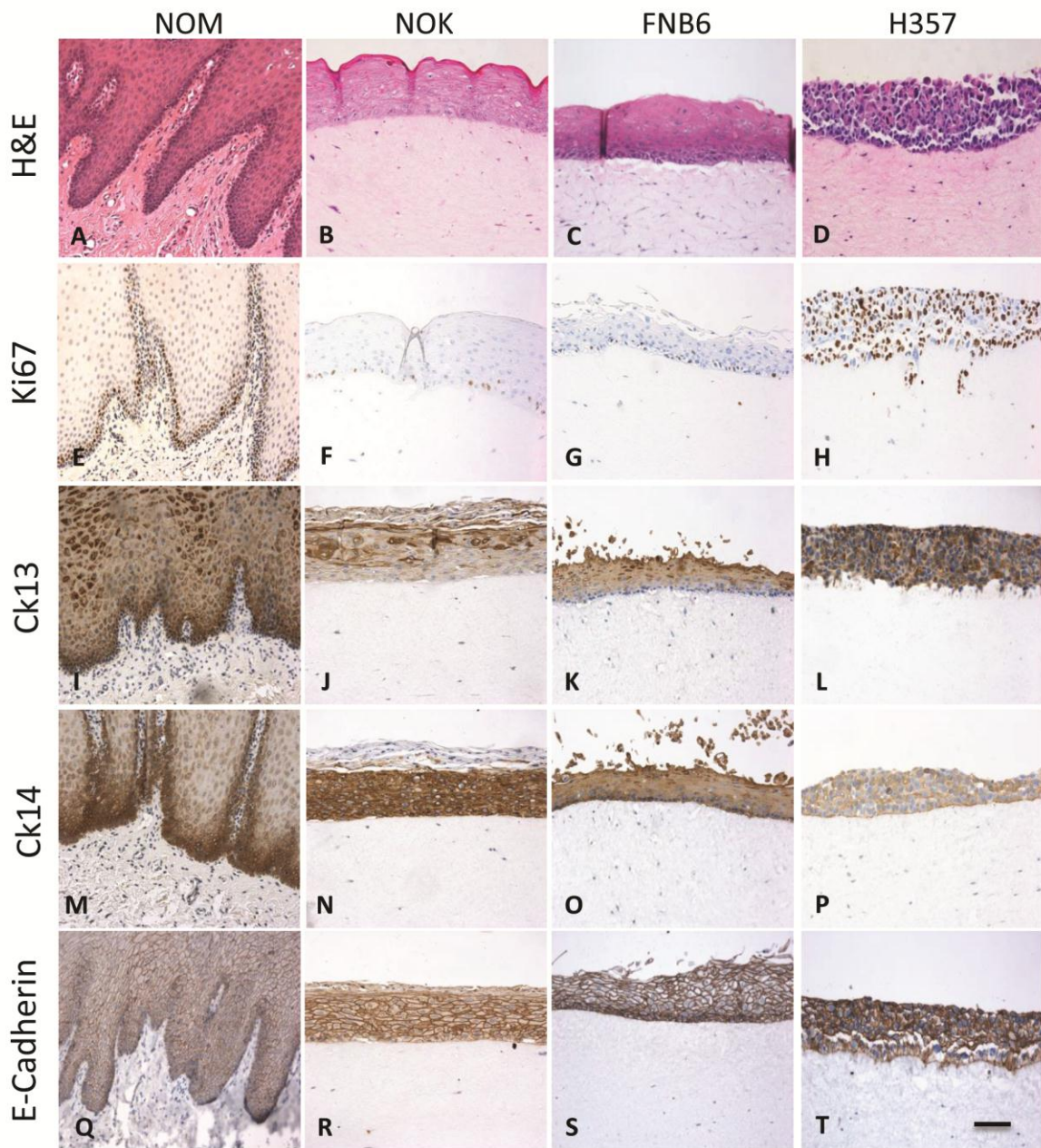


Figure 1. FNB6 OME display similar characteristics to human oral mucosa. OME were generated by culturing FNB6 or H357 cells on top of a fibroblast-populated collagen scaffold and compared to NOK-based OME and human oral mucosa. Histological (H&E) and immunohistochemical analysis for ki67, cytokeratin 13 and 14 and E-cadherin were used to characterise the models. Representative images are from three independent experiments. Scale bar = 100 μ m.

Tissue Engineering Part C: Methods
Development and characterisation of in vitro human oral mucosal equivalents derived from immortalised oral keratinocytes (doi: 10.1089/ten.TEC.2016.0310)
This article has been peer-reviewed and accepted for publication, but has yet to undergo copyediting and proof correction. The final published version may differ from this proof.
Development and characterisation of in vitro human oral mucosal equivalents derived from immortalised oral keratinocytes (doi: 10.1089/ten.TEC.2016.0310)
This paper has been peer-reviewed and accepted for publication, but has yet to undergo copyediting and proof correction. The final published version may differ from this proof.

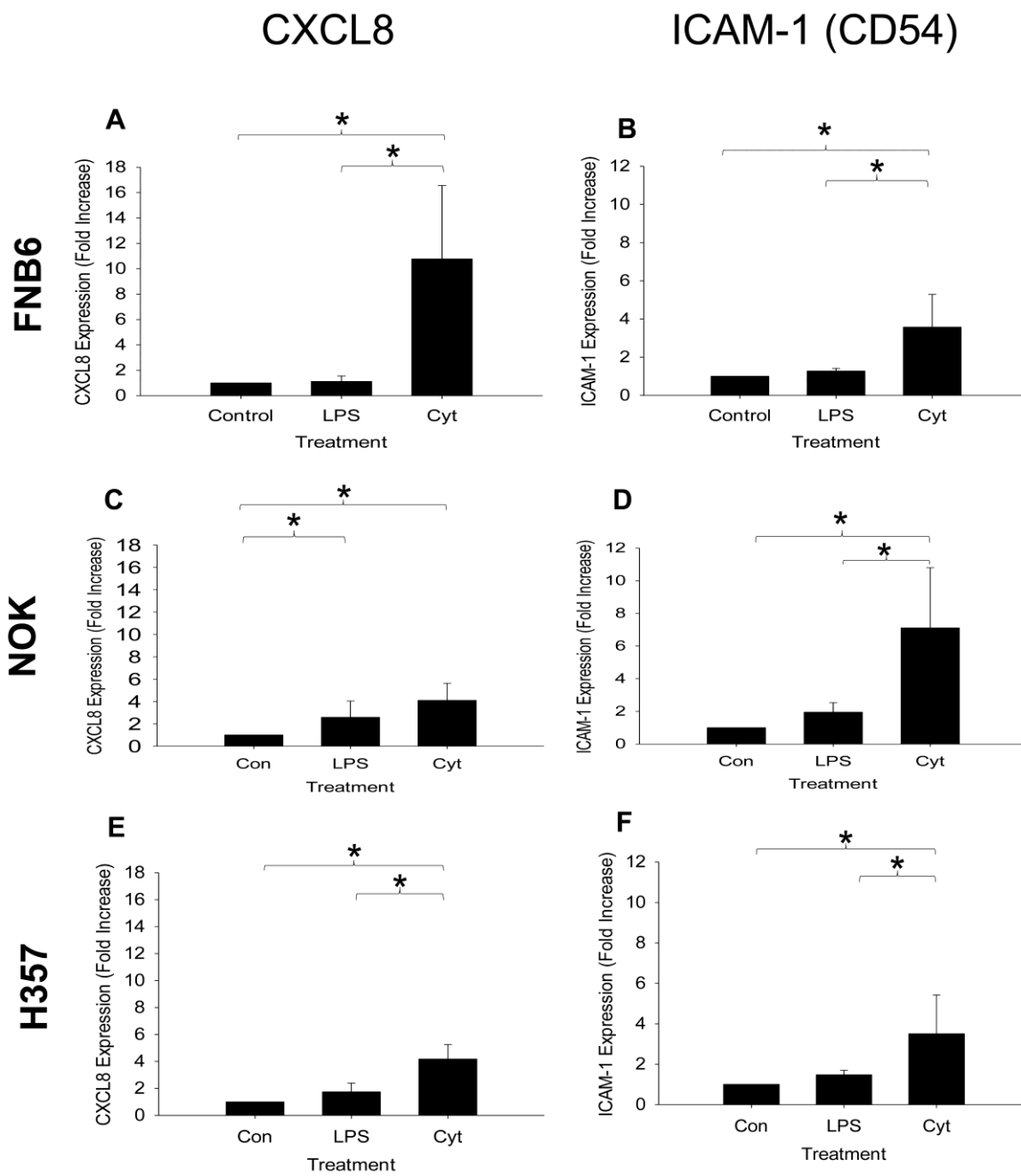


Figure 2. Gene expression of CXCL8 and ICAM-1 by FNB6 OME increases in response to stimulation. FNB6, NOK or H357 OME was stimulated with a combination of 10 ng/ml IL-1 β and 20 ng/ml TNF α , 100ng/ml *E. coli* LPS medium as control for 24 h and gene expression for CXCL8 and ICAM-1 analysed by qPCR. Data are from at least 3 independent experiments performed in triplicate. * Indicates significant difference ($p < 0.05$) from control.

Tissue Engineering Part C: Methods
Development and characterisation of in vitro human oral mucosal equivalents derived from immortalised oral keratinocytes (doi: 10.1089/ten.TEC.2016.0310)
This article has been peer-reviewed and accepted for publication, but has yet to undergo copyediting and proof correction. The final published version may differ from this proof.
Development and characterisation of in vitro human oral mucosal equivalents derived from immortalised oral keratinocytes (doi: 10.1089/ten.TEC.2016.0310)
This paper has been peer-reviewed and accepted for publication, but has yet to undergo copyediting and proof correction. The final published version may differ from this proof.

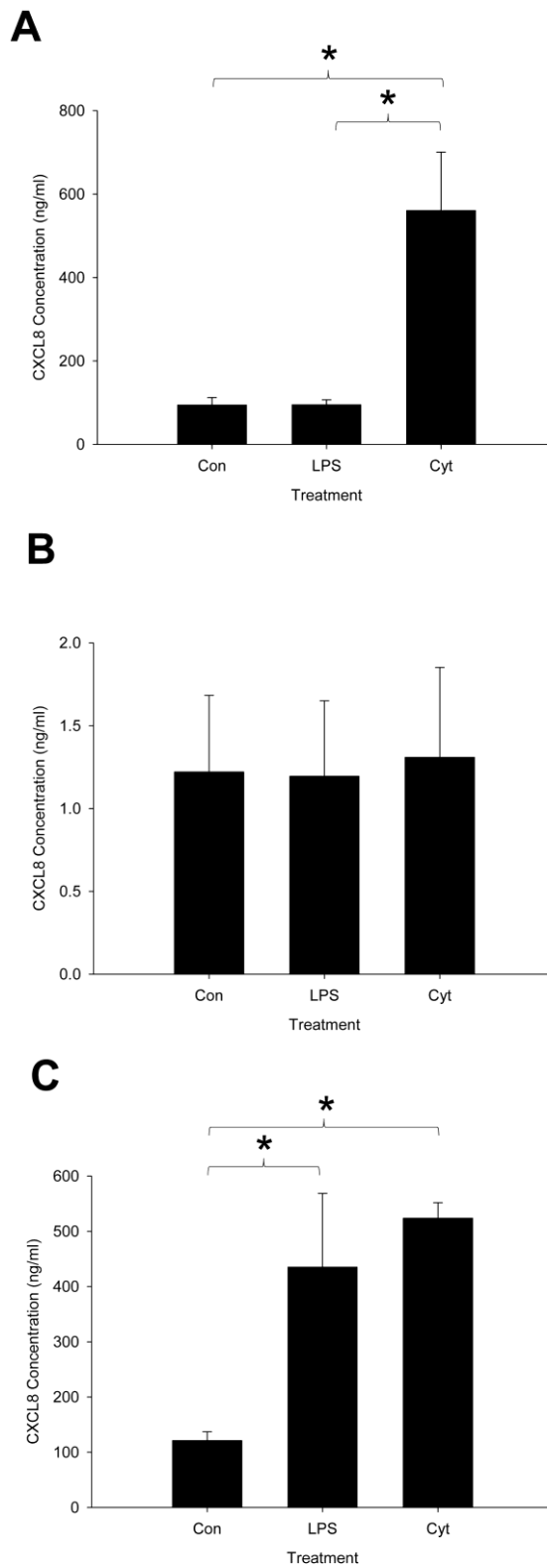


Figure 3. Protein expression of CXCL8 by FNB6 OME increases in response to stimulation.

FNB6 (A), NOK (B) or H357 (C) OME were stimulated with a combination of 10 ng/ml IL-1 β

and 20 ng/ml TNF α , 100 ng/ml *E. coli* LPS medium as control for 24 h and protein expression for CXCL8 analysed by ELISA. Data are from at least 3 independent experiments performed in triplicate. * Indicates significant difference ($p<0.05$) from control.

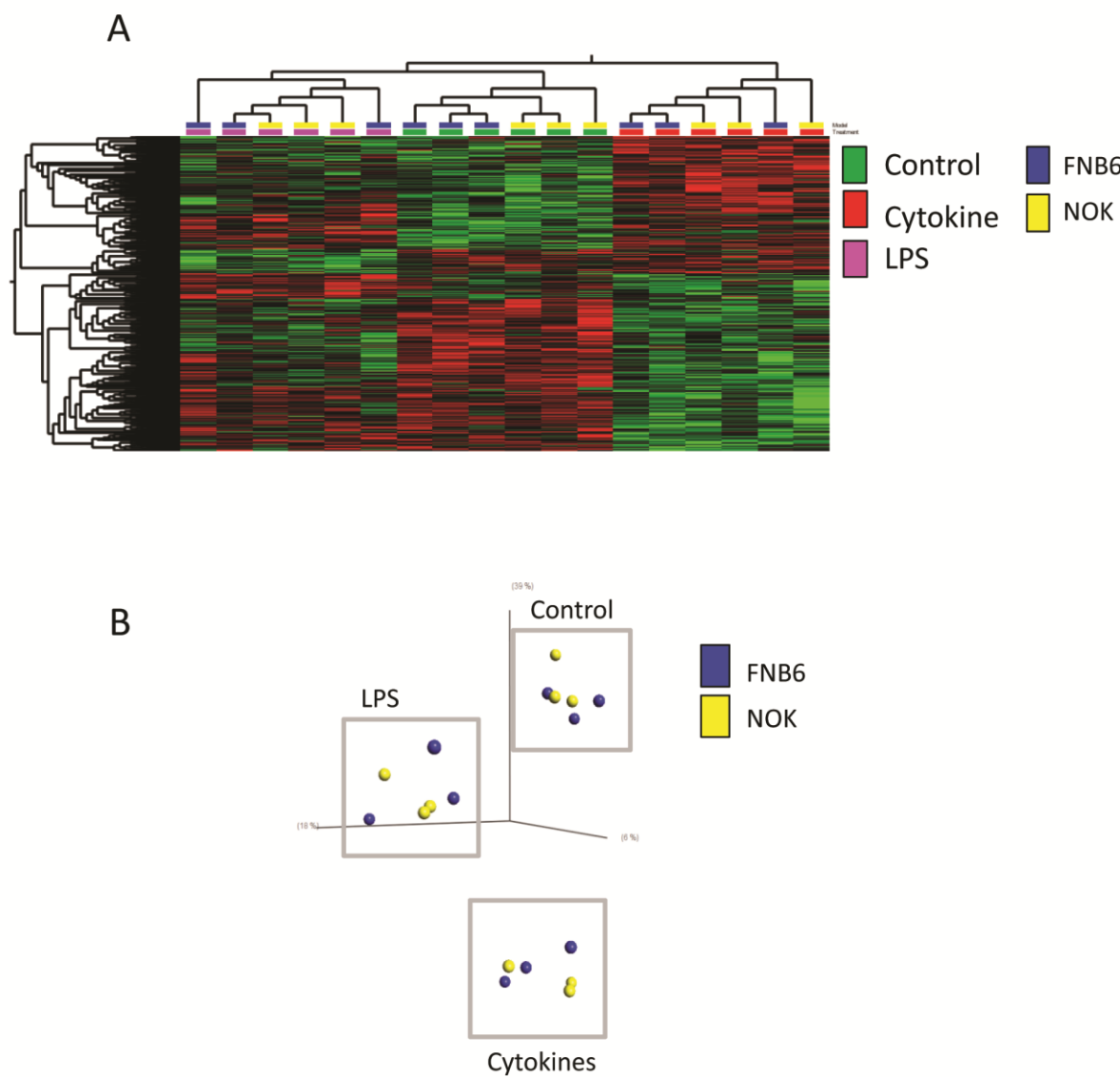


Figure 4. Whole genome expression of FNB6 and NOK OME. Heat map analysis of microarray gene analysis of FNB6 and NOK OME stimulated with a combination of 10 ng/ml IL-1 β and 20 ng/ml TNF α , 100 ng/ml *E. coli* LPS medium as control for 24 h (up-regulated genes in green and down-regulated genes in red; A). Principle Component Analysis of whole genome responses for cytokine, LPS-treated compared to medium control (B). Data are from at least 3 independent experiments. Array data show genes significantly ($p < 0.05$) affected compared to control.

Tissue Engineering Part C: Methods
Development and characterisation of in vitro human oral mucosal equivalents derived from immortalised oral keratinocytes (doi: 10.1089/ten.TEC.2016.0310)
This article has been peer-reviewed and accepted for publication, but has yet to undergo copyediting and proof correction. The final published version may differ from this proof.
Development and characterisation of in vitro human oral mucosal equivalents derived from immortalised oral keratinocytes (doi: 10.1089/ten.TEC.2016.0310)
This paper has been peer-reviewed and accepted for publication, but has yet to undergo copyediting and proof correction. The final published version may differ from this proof.

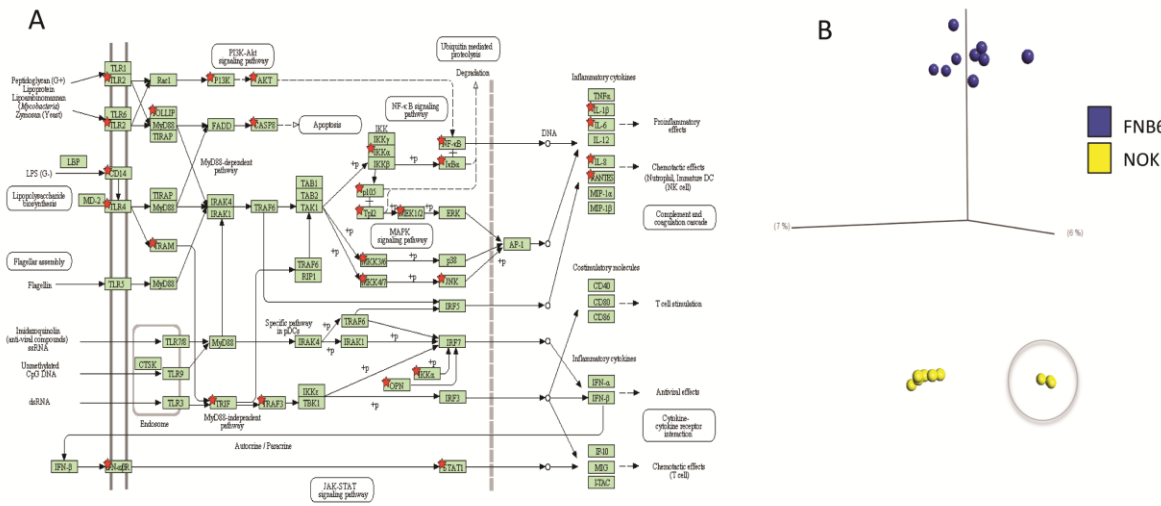


Figure 5. Activation of signal transduction pathways is similar in FNB6 and NOK OME.

Signal transduction pathway data analysis (DAVID) from the gene data for FNB6 OME show up-regulation for genes in the NF κ B pathway (A). Principle Component Analysis of whole genome responses for FNB6 compared to NOK OME showing batch-to-batch variability in gene responses between the models (B).

Table 1. Details of antibodies used for immunohistochemistry.

Name	Clone	Company	Working concentration ($\mu\text{g/ml}$)
Ck13	AE8	ThermoScientific	1.0
Ck14	LL002	ThermoScientific	0.3
Ki67	MIB-1	DAKO	1.0
E-cadherin	EP700Y	Abcam	0.5
IgG Control	11711	R&D Systems	1.0

Table 2. Top 10 genes up-regulated by NOK-OME upon stimulation with TNF- α and IL-1 β .

Gene	Fold-Change	p-value
TNFAIP6	14.07	0.0038
CXCL10	13.51	0.0198
CXCL11	9.43	0.0463
VNN1	6.31	0.0029
CCL20	6.20	0.0001
IL36G	6.02	0.0080
OLR1	5.32	0.0188
CXCL8	5.14	0.0039
S100A7A	5.13	0.0187
IL6	4.86	0.0005